



# High-Speed Synthesis of Rice-Ear-Shaped Cu Dendritic Particles at Room Temperature via Galvanic Displacement Using Zn Particles

Jun Ho Hwang<sup>1</sup> · Jong-Hyun Lee<sup>1</sup>

Received: 11 May 2018 / Accepted: 29 August 2018 / Published online: 17 September 2018  
© The Korean Institute of Metals and Materials 2018

## Abstract

Rice-ear-shaped Cu dendritic particles were fabricated via fast galvanic displacement reactions for 3–5 min under ambient conditions by adding Zn particles into an aqueous electrolyte without chloride ions. The obtained Cu dendritic particles have a small average size (4.44  $\mu\text{m}$ ) and short, multiple branches that seemed to be aggregates of nanoparticles formed on stem-like backbones, and their surface area is large. The prepared Cu dendrites could be protected against oxidation during drying via post-treatment with chelating or complexing agents. While the dendrite stem is found to be a Cu polycrystal grown only on the (111) plane, the branches consist of three planes of Cu, viz., (111), (200), and (220), indicating that they were formed by random attachment of nanoparticles and aggregates. A possible low-temperature and high-speed synthesis mechanism is proposed based on the results of time-dependent SEM investigations as well as the crystal structure of the dendrites. This novel technique to synthesize modified dendrites is extremely simple and suitable for mass production.

**Keywords** Cu dendritic particle · Rice-ear-shape · Galvanic displacement reaction · Dendritic growth · Post-treatment

## 1 Introduction

Metal dendrite powders have received much attention owing to their unique physical and chemical properties [1–16]. These powders have attractive nanostructures with large surface areas similar to nano-sized materials, despite being in the form of micro-sized particles that are easy to handle. Hence, they are highly desirable for use in electrodes [7, 9], sensors [12], catalysts [15, 16], and nanofluids [17] and have been used in electromagnetic interference shielding and conductive pastes because the electrical percolation threshold is met more easily with the dendrite filler, and thus, they can be used in smaller amounts [18, 19]. In particular, Cu powders have been widely studied and used in many applications owing to their conductive, catalytic, and optical properties [20–25]. They have even been considered as an alternative for Ag because they provide equivalent conductivity at a lower cost [26–29]. Thus, Cu dendrites have

been increasingly researched for the discovery of unusual properties as well as their potential applications [30–46].

Cu dendrites are generally synthesized by electrochemical processes [30, 31, 35–37, 42, 43, 47], electroless processes [33, 34, 40, 44–46], and hydrothermal approaches [32, 38, 39, 41]. The electroless processes are the most simple and effective, and of these, galvanic displacement reactions are considered the most representative electroless processes. The  $\text{Cu}^{2+}$  ions in an aqueous medium are displaced through reaction with a metal with a lower standard reduction potential, forming Cu dendrites under well-established conditions [33, 40, 44–46]. Yan and Xue [33] synthesized Cu dendritic structures at 120 °C over 4–18 h using a Zn foil to displace Zn with  $\text{Cu}^{2+}$  in a  $\text{CuCl}_2$  aqueous solution via a modified (hydrothermal-assisted) electroless strategy using an autoclave. Sun et al. [40] prepared Cu dendritic structures at room temperature as well as 60 °C by immersing a Zn foil into a  $\text{HCuCl}_2$  aqueous solution, and they successfully modified the deposition rate by adjusting the reduction potential using  $\text{HCuCl}_2$ . Zhuo et al. [46] reported the synthesis of dendritic Cu particles via displacement of Al foil by Cu ions at room temperature for 15 min in an aqueous electrolyte containing  $\text{SO}_4^{2-}$  and  $\text{Cl}^-$  ions. However, the number of irregular first branches per unit stem length was large, and thus, the dendrite shape uniformity was low [46].

✉ Jong-Hyun Lee  
pljh@snut.ac.kr

<sup>1</sup> Department of Materials Science and Engineering,  
Seoul National University of Science and Technology,  
Seoul 01811, Republic of Korea

Nevertheless, these reports fail to define the process most suitable for mass production; Cu dendrites grown on foils must be detached from the foil and collected. Thus, the number or area of foils should be increased substantially to obtain a large yield in a short production time. Moreover, foil remnants may be present as an impurity in the collected Cu dendrites. Hence, a simpler synthesis method is highly desired. Using powder instead of foil as a trigger material would increase the productivity per unit time owing to the increased reaction area, and the fabricated Cu dendrites would be far easier to collect by depletion of the Zn particles. Therefore, powder materials are highly suitable for mass production.

Here, Zn particles were used as the reducing agent in the synthesis of Cu dendrites. An aqueous electrolyte without chloride ions aided the uniform growth of the dendrites and enhanced the reproducibility by reducing the complexity of the reaction. The reaction at room temperature (25 °C) is driven by the difference between the standard reduction potentials of  $Zn^{2+}$  (−0.76 V) and  $Cu^{2+}$  (+0.34 V) in the electrolyte [33, 40]; Cu ions are reduced and Zn dissolves into the electrolyte. Our aim was to develop a fast, simple synthesis process to obtain a high yield within a few minutes without using a complex apparatus in open air under ambient conditions (room temperature and atmospheric pressure), so that it could be adapted for mass production. Additionally, post-treatment of the synthesized Cu dendrites to suppress its rapid oxidation owing to the excessive surface area is also discussed.

## 2 Experimental Procedure

To obtain dendritic particles, copper sulfate pentahydrate ( $CuSO_4 \cdot 5H_2O$ , OCI, 99.0%) was dissolved in 2 L of distilled water, and the pH was adjusted using sulfuric acid ( $H_2SO_4$ , Daejung Chemical, 98%). Then, optimal amount of a Zn powder (average size: 70  $\mu m$ , 99.9%) was added to it under stirring. The reaction was performed at room temperature under ambient pressure for a specific time. The solution was washed three times using distilled water and pure Cu dendritic particles were collected by decantation and drying.

The morphologies of the initial and remaining Zn particles as a function of reaction time were observed by scanning electron microscopy (SEM, SU8010, Hitachi), and the composition of the synthesized dendrites was determined by energy-dispersive X-ray spectrometry (EDS, Noran system 7, Thermo Fisher Scientific) and X-ray diffractometry (XRD, D8 Advance, Bruker). Observation of the morphology at high magnifications and crystallographic analyses of the synthesized Cu dendrites were performed using a transmission electron microscope (TEM, G2 F30ST, Tecnai). Samples for TEM were prepared by dropping an ethanol

dispersion of the Cu dendrites onto a formvar/carbon-coated Cu grid and drying in air.

## 3 Results and Discussion

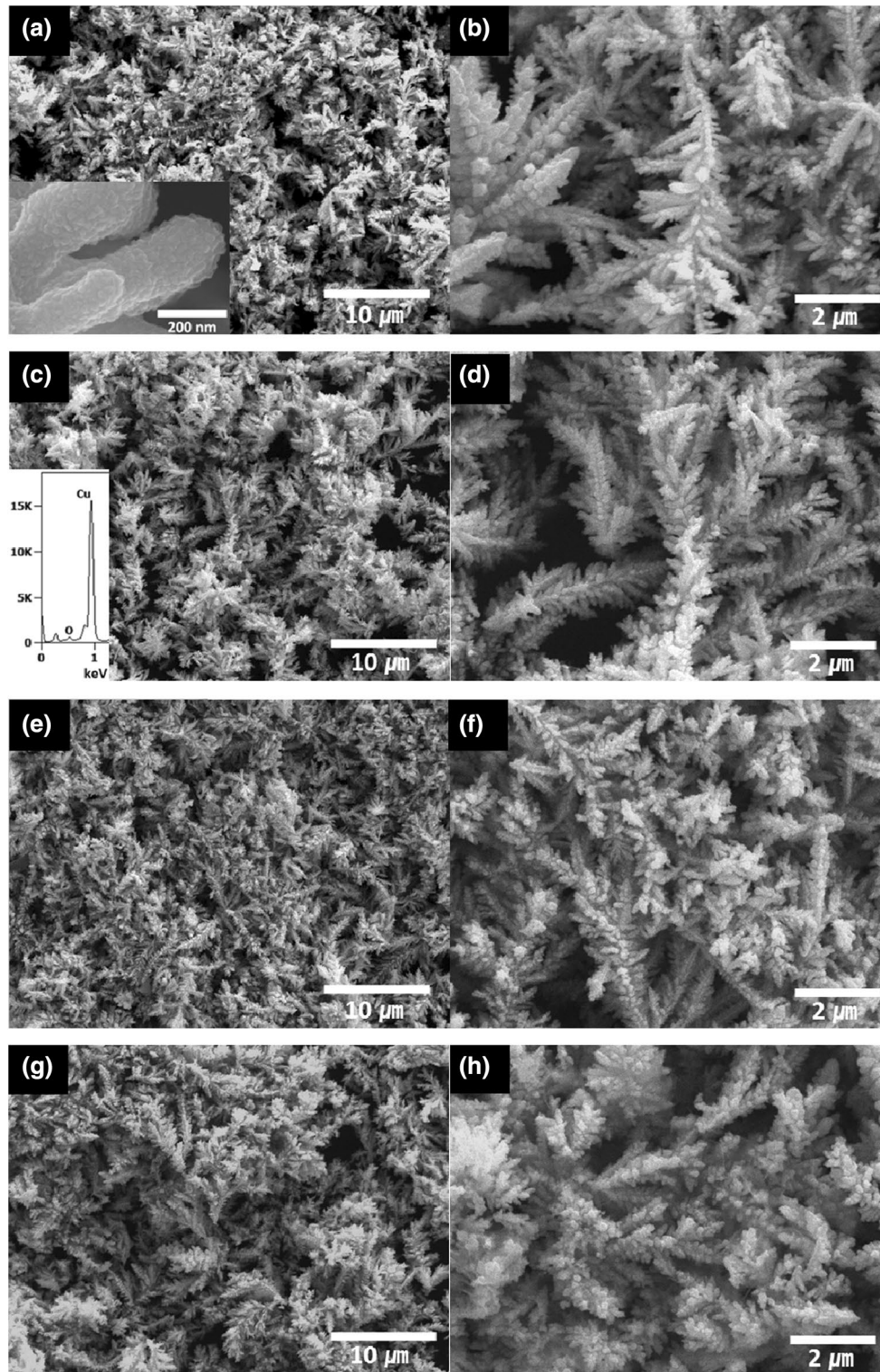
### 3.1 Microstructure Characteristics

Figure 1 shows the morphologies of the Cu dendrites synthesized for different times. The Cu solution, which was initially Prussian blue, turned transparent after approximately 3 min. This indicates that most of the Cu particles had formed within 3 min. Most of the Cu dendrites had “rice-ear” shapes, with short, multiple branches that seemed to be irregular aggregates of nanoparticles (inset of Fig. 1a) attached to a relatively long (several micrometers) stem-like backbone. The branches grew in various directions and they were scattered around the stem at oblique angles.

To eliminate the remaining Cu ions, the reaction was prolonged to 5 min. After this, the branches were found to be slightly longer and more uniform, and homogeneous dendrites were obtained in a high yield. The average length of the stems is 4.80 ( $\pm 1.42$ )  $\mu m$  and the branches have diverse lengths of 10–400 nm—these are shorter than those of other reported Cu dendrites; the bubbles generated by hydrogen evolution during the synthesis hinder the formation of long stems. The average size of the dendrites determined by the laser scattering method is 4.44  $\mu m$ . The EDS profile of the synthesized product (inset in Fig. 1c) indicates that the dendrite is composed of pure Cu. The tap density of the dendrites was found to be extremely low (1.13  $g/cm^3$ ) [48], indicating an extremely large surface area. With reaction times ranging up to 7 and 15 min, the initially formed sharp dendrites become blunt, with denser branches.

The shapes and surface morphologies of the Zn particles used in the synthesis are presented in Fig. 2. The sizes and shapes of the particles are distinctly irregular. The surface appears smooth at low magnification, because they were fabricated by atomization; however, the surface is actually rough at high magnification. A surface covered with fine irregular nodules was also observed locally. EDS analysis of the particles indicates that the particles consist of mainly Zn, with a minor oxygen peak, indicating the presence of only native oxide [49].

To investigate the growth mechanism of the Cu dendrites, their time-dependent evolution was monitored. The morphologies formed with varying short reaction times are shown in Figs. 3 and 4. The surface morphologies of the Zn particles after only 5 s of reaction are displayed in Fig. 3. Diverse Cu products had already formed on the mesa surfaces of the Zn particles: irregular aggregates (Fig. 3a), sprout-like aggregates (Fig. 3b, c), sea cucumber-like aggregates (Fig. 3b, c), and growth of rice-ear-shaped dendrites



**Fig. 1** **a, c** Low- and **b, d** high-magnification SEM images of Cu dendrites formed after different synthesis times: **a, b** 3, **c, d** 5, **e, f** 7, and **g, h** 15 min. The inset in **a** shows an enlarged image of the branch tips. The inset in **c** shows the EDS profile of the dendrites

(Fig. 3c) with extremely short branches on a relatively long stem—a different morphology to that of the final dendrites—indicating the exposure of Zn crystalline planes owing to

etching by the Cu solution. A very small amount of the detached Cu particles collected were rice-ear-shaped dendrites, whereas a large amount of it consisted of irregular

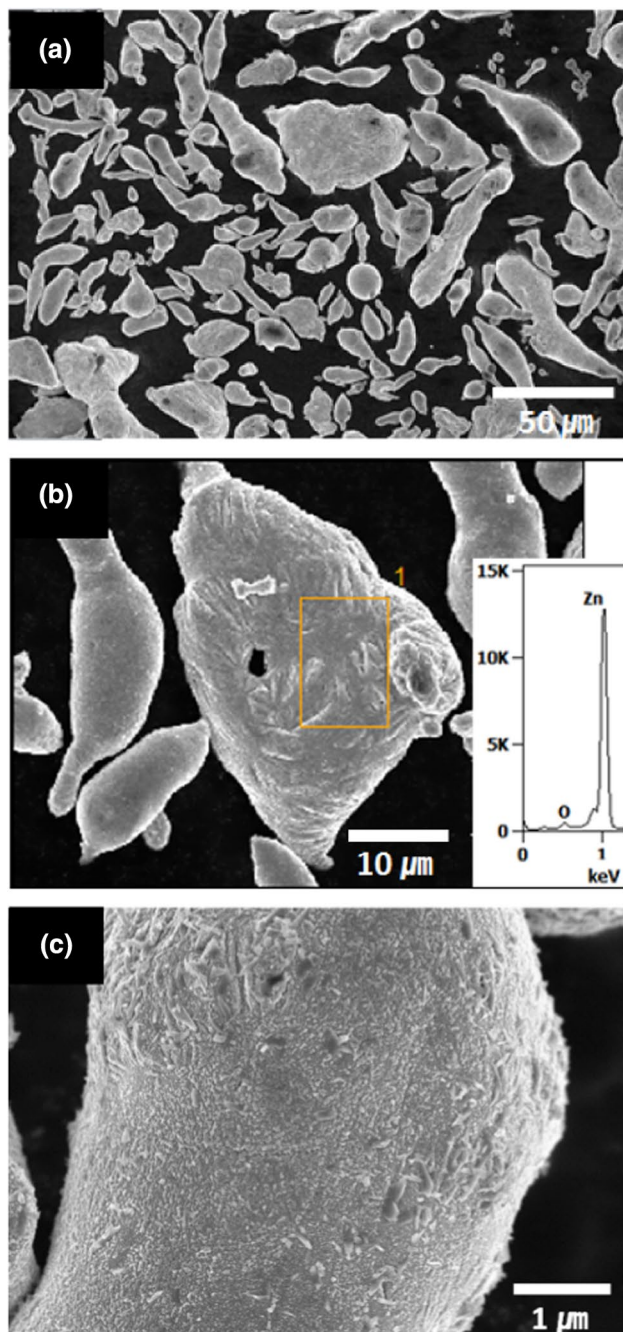


**Fig. 2** **a, b** Low- and **c** high-magnification SEM images at different magnifications showing the initial state of the used Zn particles. The inset in **b** shows the EDS profile of the Zn particle

aggregates and sea cucumber-like structures that had not grown into dendrites.

The fact that Cu dendrites can be formed within 5 s represents an extremely rapid synthesis using our system. For the synthesis of metal dendrites via galvanic displacement, three preconditions are required: large size ( $> 5 \mu\text{m}$ ) of the added particle, high concentration ( $> 5 \text{ mM}$ ) of the starting Cu(II) species, and fast growth rate of the synthesized metal

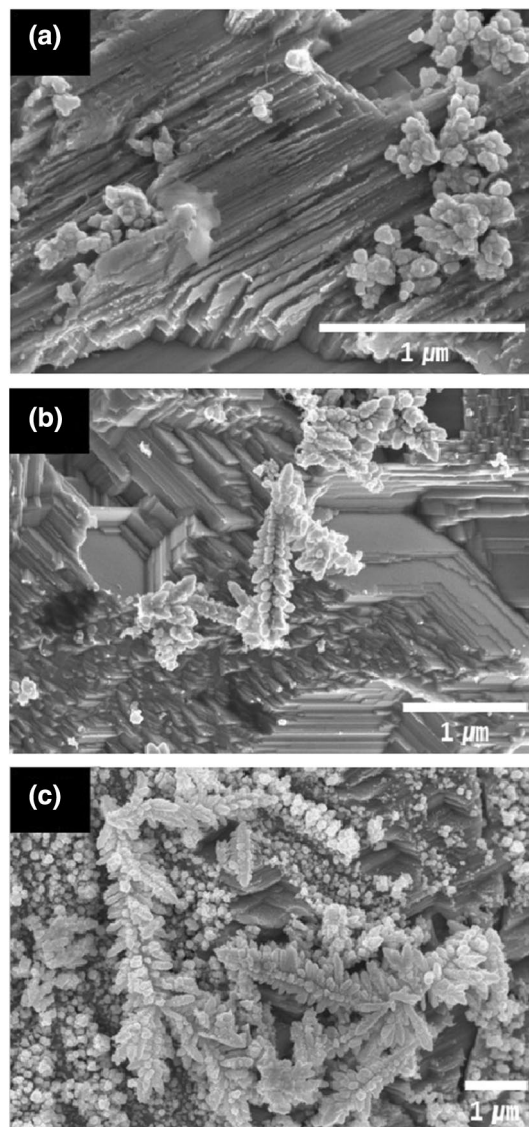


**Fig. 3** **a, b, c** SEM images of Zn particles collected immediately after a reaction time of 5 s

[50]. The current synthesis of dendrites is judged to satisfy these preconditions. The morphological changes in the Zn particles imply that the Zn atoms vigorously dissolve into the solution as  $\text{Zn}^{2+}$  ions, thus donating electrons. Then, the electrons are immediately accepted by  $\text{Cu}^{2+}$  ions and  $\text{O}_2$ , thus leading to the deposition of heterogeneous Cu nuclei on the surface of Zn with the formation of  $4\text{OH}^-$  ions [33, 40].

The morphologies of the Cu particles collected immediately after different reaction times are displayed in Fig. 4. The structures of the Cu particles collected after 5 and 10 s can be distinguished into three types: irregular aggregates from several tens of nanometers to one micrometer in size, sea cucumber-like structures from submicrometer to several micrometers in length, and the rice-ear-shaped

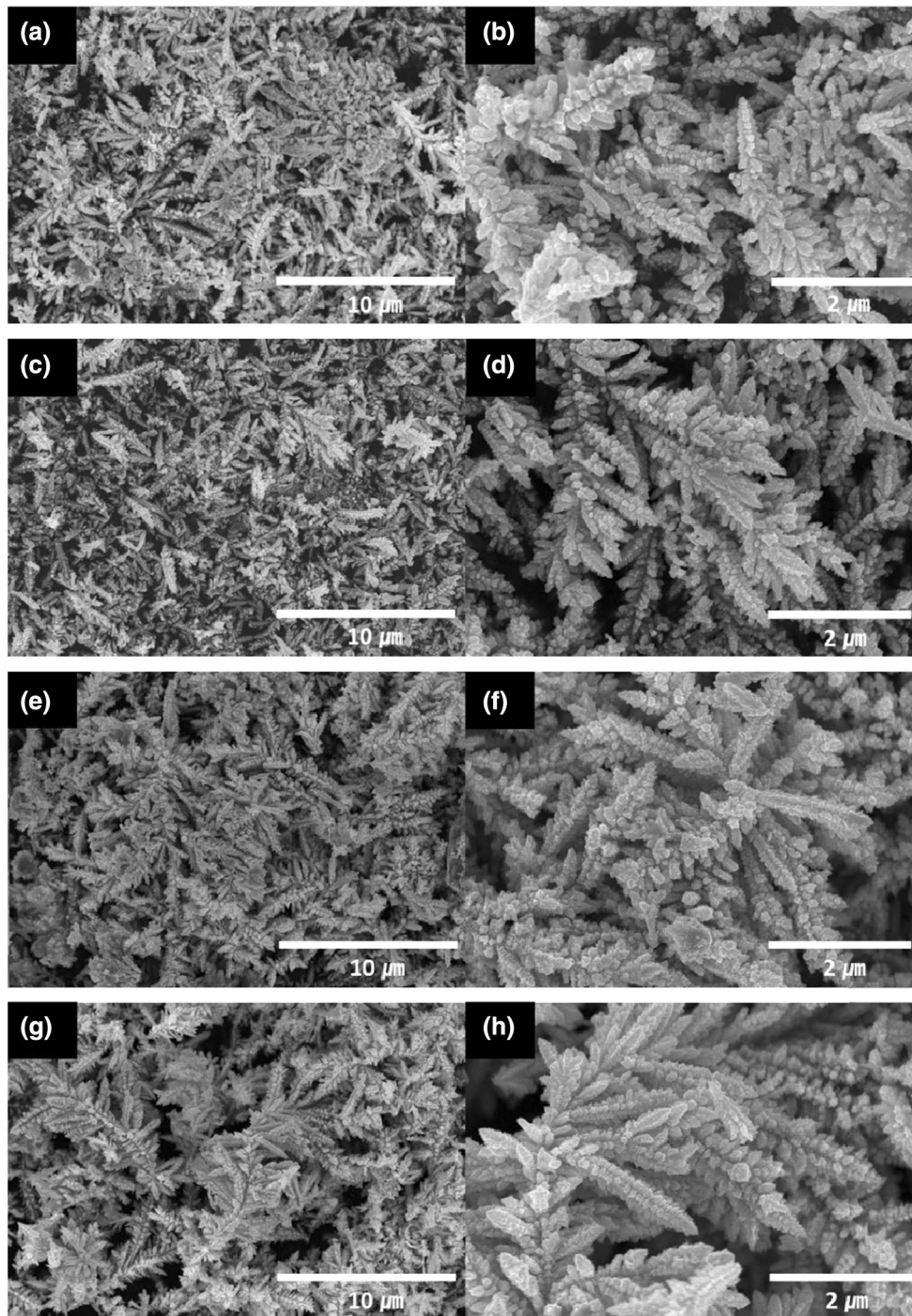


**Fig. 4** **a, c, e, g** Low- and **b, d, f, h** high-magnification SEM images of Cu particles collected immediately after different reaction times: **a, b** 5, **c, d** 10, **e, f** 30, and **g, h** 60 s

dendrites. As the reaction time is increased to 30 s, the sea cucumber-like structures are transformed into rice-ear-shaped dendrites, with the development of branches together with longitudinal and radial growth of the stem.

As the reaction time is increased to 60 s, the dendrites show a more branch-rich morphology and the total volume of the Zn particles decreases, indicating lasting dissolution of Zn.

### 3.2 Effect of Post-treatment

Some dendrites were then post-treated by rinsing three times with an aqueous solution of ethylenediaminetetraacetic acid (EDTA,  $C_{10}H_{16}N_2O_8$ , Samchun Pure Chemical, 99.0%) or benzotriazole ( $C_6H_5N_3$ , Daejung Chemical, 98.5%) through centrifugation at 250 rpm for 3 min. The SEM images and XRD patterns of the resultant particles are displayed in Fig. 5. All three samples show identical peaks corresponding to the (111), (200), and (220) planes of face-centered cubic (fcc) Cu (JCPDS file no. 04-0836), detected at  $2\theta = 43.3^\circ$ ,  $50.4^\circ$ , and  $74.1^\circ$ , respectively, with a slight peak shift to lower angles. The shift seems to occur owing to slight expansion of the lattices in the nanostructures formed due to random attachment/deposition of Cu. However, the  $Cu_2O$  peak is detected at  $36.4^\circ$  only in the non-treated sample, implying that the oxidation of the Cu dendrites is suppressed after the post-treatment. EDTA is easily ionized in distilled water. The ionized EDTA chelates with the Cu ions, thus eliminating the remaining Cu ions on the surface of dendrites [51]. Hence, the oxidation of the Cu ions at the surface can be suppressed. Benzotriazole also ionizes in distilled water, and the ionized benzotriazole complexes with the Cu ions on the surface of the dendrites, thus forming a protective layer [52]. The layer also effectively suppresses the surface oxidation.

### 3.3 Crystallographic Characteristics

TEM images of the as-synthesized Cu dendrites are presented in Fig. 6. To elucidate the crystalline states of the stem and branches, fast Fourier transformation (FFT) patterns, taken at locations A (stem) and B (branch) in Fig. 6a, are analyzed in detail in Fig. 6b. In the stem region, the lattice spacing is calculated to be  $2.103 \text{ \AA}$ , which agrees with the (111) lattice spacing of bulk Cu ( $2.087 \text{ \AA}$ ) [33, 34], and in the branch region, lattice spacings of  $1.872$  and  $1.274 \text{ \AA}$  are found, which could be attributed to the (200) and (220) planes of Cu (JCPDS file no. 85-1326). In the high-resolution TEM image in Fig. 6c, the interface between the stem and deviational branches has a distinct boundary, which implies that the stem and branches have different growth planes. Furthermore, the lattice fringes in the stem are not regular, with different fringe spacings such as  $0.208$  and  $0.212 \text{ nm}$  (with respect to location), although both are closest to the (111) lattice spacing of Cu. Similar irregular lattice fringes and spacings are also observed in the high-resolution image of the branch tips. Fringe spacings of  $0.209$ ,  $0.181$ , and  $0.128 \text{ nm}$ —corresponding to (111), (200), and (220) lattice spacings, respectively—are observed together in a branch tip, as shown in Fig. 6d. Therefore, stems and branches can be concluded to be polycrystalline, unlike the results of previous reports [33, 34, 40, 44, 45], with stems made of only (111) planes and branches consisting of three

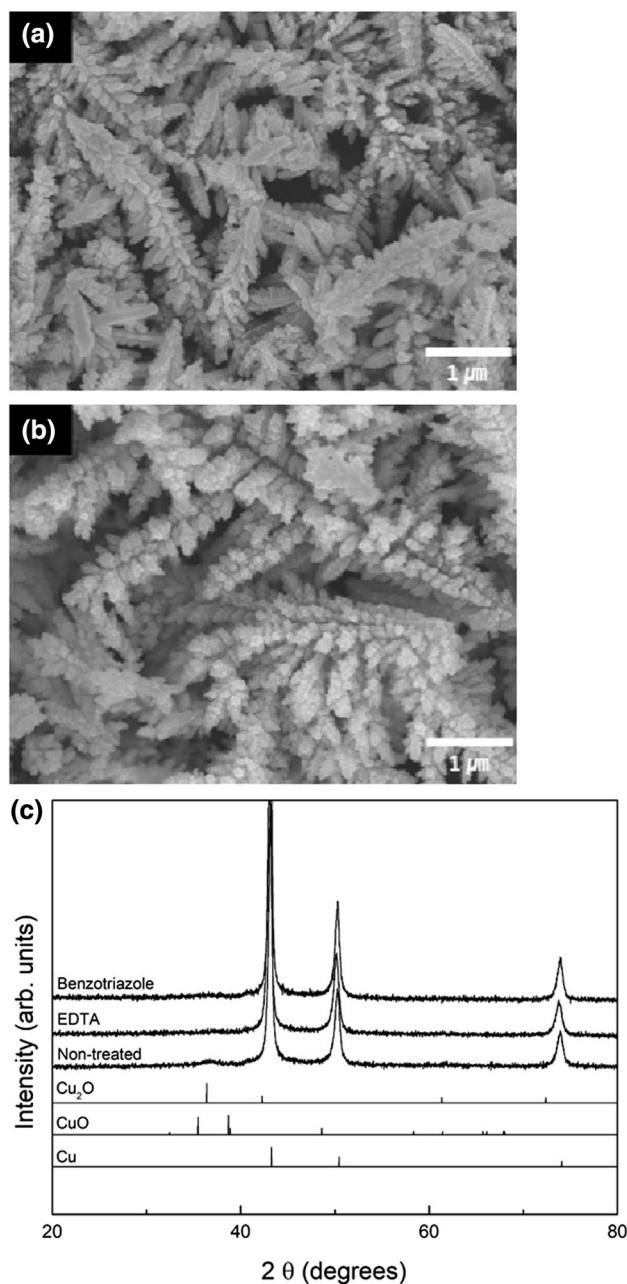


**Fig. 5** SEM images of Cu dendrites post-treated with **a** EDTA and **b** benzotriazole solutions and **c** the corresponding XRD patterns

planes, indicating a nanoparticle-aggregation process. These results corroborate the above XRD analysis. The stems grow rapidly through Cu attachment and deposition on the close-packed fcc (111) surfaces of the initial Cu seeds, which have a high surface energy. This is followed by rapid branch growth, where mechanisms such as selective deposition [44, 53], fractal growth [33, 34, 44, 54], and oriented attachment of nanoparticles [33, 40, 45] no longer occurred. In summary, the high-speed fabrication in this study compared with other dendrite synthesis is achieved by the rapid formation of

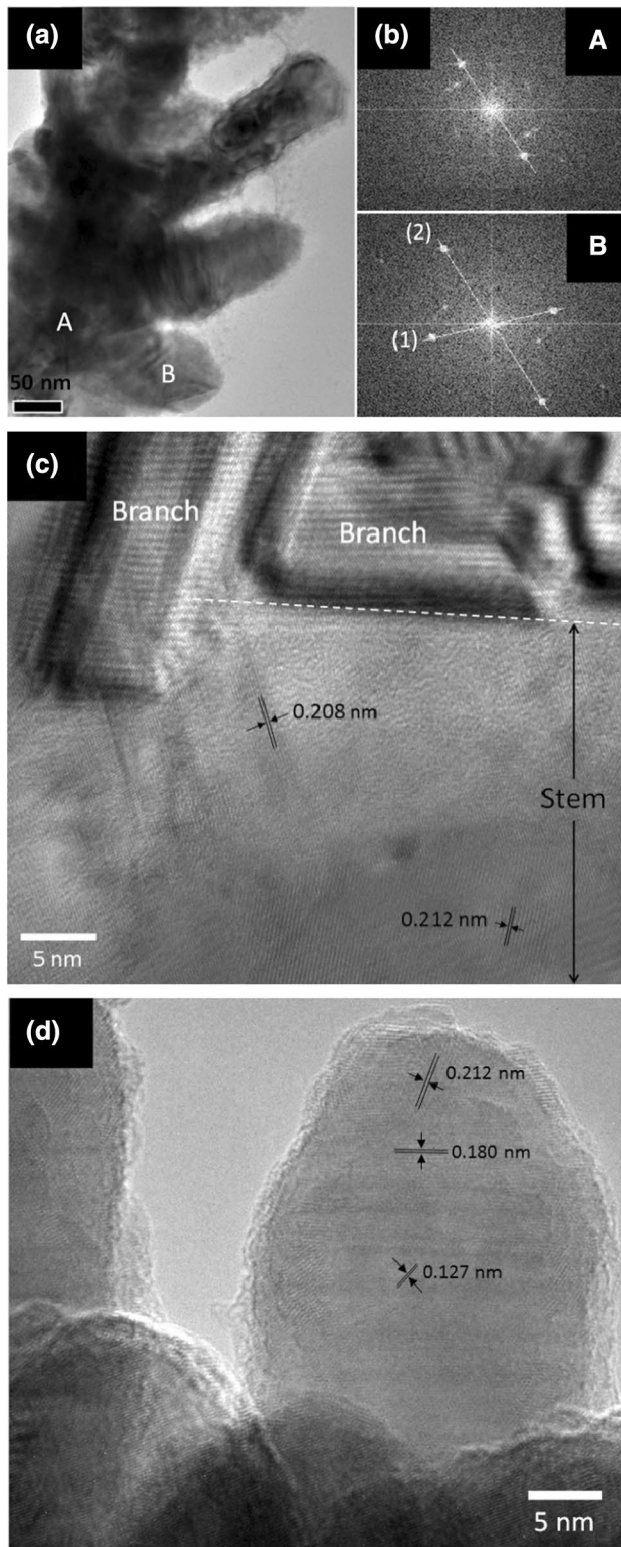


**Fig. 6** **a** TEM image of a typical as-synthesized Cu dendrite. **A** and **B** show the FFT patterns of regions marked with letters **A** and **B** in **b**. High-resolution TEM images of the dendritic structure showing **c** the interface between a stem and branch and **d** a branch tip

branches with the aid of random attachment of nanoparticles through the extremely fast galvanic displacement reaction.

The dendritic shapes are formed by the phenomena of nonequilibrium growth [55]. The Zn particles dissolve in the  $\text{CuSO}_4/\text{H}_2\text{SO}_4$  solution and the Cu nuclei are generated. Once  $\text{Cu}^{2+}$  ions contact the surface of a Zn particle, they pick up electrons and are deposited onto the Zn particle, forming a nucleus. Further  $\text{Cu}^{2+}$  ions attach to this nucleus, forming a cluster on the surface. These processes explain the (111)-oriented growth of stems. Simultaneously, Cu nuclei that form in the solution aggregate to form larger clusters (tiny nanoparticles). Owing to the low reaction temperature, the rate of mass transport (diffusion) of the nuclei will be low, thus the aggregation can proceed briskly. The Cu nanoparticles move randomly under Brownian motion; some of them are attached randomly onto the Zn surface, whereas others coalesce into larger aggregates, and are also eventually attached to the surface. Under the diffusion-limited aggregation model [33, 40, 56], the rapid increase in the number of nuclei induced by the addition of Zn particles accelerates the formation of aggregates by collision between the nanoparticles, resulting in a dendritic structure with short branches. The nanoparticles and aggregates attach onto the surface of a stem and are then converted into more crystalline structures while being sintered through diffusion, finally forming a polycrystalline structure.

## 4 Conclusions

A fast and simple method for the synthesis of Cu dendrites under ambient conditions is developed by adding Zn particles into an aqueous electrolyte without chloride ions. Cu dendritic particles with an average size of  $4.44 \mu\text{m}$ , shaped like rice ears, were uniformly fabricated through galvanic displacement reactions after a short synthesis time of 3–5 min. The backbone stems have an average length of  $4.80 \mu\text{m}$  and they are polycrystals grown only along the (111) plane. The short, multiple branches formed on the backbone stems seemed to be aggregates of nanoparticles and consisted of three planes (111), (200), and (220). The synthesis mechanism was discussed in accordance with the results of time-dependent SEM investigations and TEM studies used to observe the detailed structure of the dendrite. Post-treatment techniques for suppressing rapid oxidation during drying, owing to the excessive surface area, was also discussed.

**Acknowledgements** This work was supported by the Nano-Convergence Foundation ([www.nanotech2020.org](http://www.nanotech2020.org), Grant No. R201703410) funded by the Ministry of Science, ICT and Future Planning (MSIP, Korea) and the Ministry of Trade, Industry and Energy (MOTIE, Korea) [Project Name: Commercialization of 100 Gbps optical receiver and transmitter modules based on nano Ag-coated Cu paste]. The

authors also thank the Korean Basic Science Institute (KBSI) for the TEM analysis.

**Funding** Funding was provided by Nano-Convergence Foundation (Grant No. R201703410).

## References

- J.P. Xiao, Y. Xie, R. Tang, M. Chen, X.B. Tian, *Adv. Mater.* **13**, 1887 (2001)
- K.D. Kim, K.Y. Choi, H.T. Kim, *Scr. Mater.* **53**, 571 (2005)
- J.X. Fang, X.N. Ma, H.H. Cai, X.P. Song, B.J. Ding, *Nanotechnology* **17**, 5841 (2006)
- J.X. Fang, B.J. Ding, X.P. Song, *Appl. Phys. Lett.* **91**, 083108 (2007)
- X.-M. Liu, S.-Y. Fu, *J. Cryst. Growth* **306**, 428 (2007)
- L.-P. Zhu, H.-M. Xiao, W.-D. Zhang, Y. Yang, S.-Y. Fu, *Cryst. Growth Des.* **8**, 1113 (2008)
- N. Zhao, Y. Wei, N. Sun, Q. Chen, J. Bai, L. Zhou, Y. Qin, M. Li, L. Qi, *Langmuir* **24**, 991 (2008)
- J. Ye, Q.-W. Chen, H.-P. Qi, N. Tao, *Cryst. Growth Des.* **8**, 2464 (2008)
- T. Huang, F. Meng, L. Qi, *Langmuir* **26**, 7582 (2010)
- Y.-J. Song, J.-Y. Kim, K.-W. Park, *Cryst. Growth Des.* **9**, 505 (2009)
- X. Chen, C.-H. Cui, Z. Cuo, J.-H. Liu, X.-J. Huang, S.-H. Yu, *Small* **7**, 858 (2011)
- H.-B. Noh, K.-S. Lee, P. Chandra, M.-S. Won, Y.-B. Shim, *Electrochim. Acta* **61**, 36 (2012)
- J.Y. Zheng, Z.L. Quan, G. Song, C.W. Kim, H.G. Cha, T.W. Kim, W. Shin, K.J. Lee, M.H. Jung, Y.S. Kang, *J. Mater. Chem.* **22**, 12296 (2012)
- H. Chen, C. Xu, X. Zhou, Y. Liu, G. Zhao, *Mater. Res. Bull.* **47**, 4353 (2012)
- J. Rosen, G.S. Hutchings, Q. Lu, R.V. Forest, A. Moore, F. Jiao, *ACS Catal.* **5**, 4586 (2015)
- J. Choi, M.J. Kim, S.H. Ahn, I. Choi, J.H. Jang, Y.S. Ham, J.J. Kim, S.-K. Kim, *Chem. Eng. J.* **299**, 37 (2016)
- S.Y. Lee, S.H. Jin, S.M. Kim, J.W. Kim, *Met. Mater. Int.* **20**, 695 (2014)
- R.K. Goyal, K.R. Kambale, S.S. Nene, B.S. Selukar, S. Arbu, U.P. Mulik, *Mater. Chem. Phys.* **128**, 114 (2011)
- C. Yang, X. Cui, Z. Zhang, S.W. Chiang, W. Lin, H. Duan, J. Li, F. Kang, C.-P. Wong, *Nat. Commun.* **6**, 8150 (2015)
- S.K. Kand, S. Purushothaman, *J. Electron. Mater.* **28**, 1314 (1999)
- M. Joo, B. Lee, S. Jeong, M. Lee, *Appl. Surf. Sci.* **258**, 521 (2011)
- N. Toshima, Y. Wang, *Langmuir* **10**, 4574 (1994)
- R. Reske, H. Mistry, F. Behafarid, B.R. Cuenya, P. Strasser, *J. Am. Chem. Soc.* **136**, 6978 (2014)
- H.H. Huang, F.Q. Yan, Y.M. Kek, C.H. Chew, G.Q. Xu, W. Ji, P.S. Oh, S.H. Tang, *Langmuir* **13**, 172 (1997)
- S.S. Joshi, S.F. Patil, V. Iyer, S. Mahumuni, *Nanostruct. Mater.* **10**, 1135 (1998)
- Y. Kobayashi, T. Shirochi, Y. Yasuda, T. Morita, *Solid State Sci.* **13**, 553 (2011)
- T. Ishizaki, R. Watanabe, *J. Mater. Chem.* **22**, 25198 (2012)
- T. Yamakawa, T. Takemoto, M. Shimoda, H. Nishikawa, K. Shiokawa, N. Terada, *J. Electron. Mater.* **42**, 1260 (2013)
- X. Liu, H. Nishikawa, *Scr. Mater.* **120**, 80 (2016)
- H. Lui, X. Zhao, Q. Fu, *Solid State Commun.* **140**, 9 (2006)
- H. Liu, X. Zhao, *Appl. Phys. Lett.* **90**, 191904 (2007)
- X. Zhang, G. Wang, X. Liu, H. Wu, B. Fang, *Cryst. Growth Des.* **8**, 1430 (2008)
- C. Yan, D. Xue, *Cryst. Growth Des.* **8**, 1849 (2008)
- Z. Ji, H. Li, Y. Liu, W. Hu, Y. Liu, *Nanotechnology* **19**, 135602 (2008)
- W.B. Shao, G. Zangari, *J. Phys. Chem. C* **113**, 10097 (2009)
- R. Qui, H.G. Cha, H.B. Noh, Y.B. Shim, X.L. Zhang, R. Qiao, D. Zhang, Y.I. Kim, U. Pal, Y.S. Kim, *J. Phys. Chem. C* **113**, 15891 (2009)
- M.S. El-Genk, A.F. Ali, *J. Heat Transf.* **132**, 071501 (2010)
- Z.Y. Zhang, C.G. Hu, B. Feng, C.H. Zheng, X.S. He, X. Wang, *J. Supercond. Nov. Magn.* **23**, 893 (2010)
- Y. Zheng, Z. Zhang, P. Guo, P. He, Z. Sun, *J. Solid State Chem.* **184**, 2114 (2011)
- S. Sun, C. Kong, L. Wang, S. Yang, X. Song, B. Ding, Z. Yang, *Cryst. Eng. Commun.* **13**, 1916 (2011)
- Q.D. Truong, M. Kakihana, *J. Cryst. Growth* **348**, 65 (2012)
- A. Taleb, Y. Xue, *Electrochim. Acta* **112**, 838 (2013)
- H. Jung, S.H. Lee, J. Yang, M. Cho, Y. Lee, *RSC Adv.* **4**, 47714 (2014)
- H.H. Nersisyan, Y.-J. Lee, S.-H. Joo, S.K. Han, T.-H. Lee, J.-S. Lee, Y.-S. An, J.-H. Lee, *Cryst. Eng. Commun.* **17**, 7535 (2015)
- R. Bakhavatsalam, S. Ghosh, R.K. Biswas, A. Saxena, A. Raja, M.O. Thotiyil, S. Wadhai, A.G. Banpurkar, J. Kundu, *RSC Adv.* **6**, 8416 (2016)
- K. Zhuo, C.Y. An, P.K. Kannan, N. Seo, Y.-S. Park, C.-H. Chung, *Korean J. Chem. Eng.* **34**, 1483 (2017)
- T.N. Huan, G. Rousse, S. Zanna, I.T. Lucas, X. Xu, N. Menguy, V. Mougel, M. Fontecave, *Angew. Chem.* **129**, 4870 (2017)
- K. Nishiyabu, in *Some Critical Issues for Injection Molding*, ed. by J. Wang (InTech, Rijeka, 2012), p. 105
- J. Zuo, A. Erbe, *Phys. Chem. Chem. Phys.* **12**, 11467 (2010)
- R. Liu, A. Sen, *Chem. Mater.* **24**, 48 (2012)
- J.E. Brown, H. Khodr, R.C. Hider, C.A. Rice-Evans, *Biochem. J.* **330**, 1173 (1998)
- M. Finšgar, I. Milošev, *Corros. Sci.* **52**, 2737 (2010)
- Y. Yang, Q. Zhang, Z.-W. Fu, D. Qin, *A.C.S. Appl. Mater. Interfaces* **6**, 3750 (2014)
- R.M. Brady, R.C. Ball, *Nature* **309**, 225 (1984)
- M. Matsushita, M. Sano, Y. Hayakawa, H. Honjo, Y. Sawada, *Phys. Rev. Lett.* **53**, 286 (1984)
- T.A. Witten Jr., L.M. Sander, *Phys. Rev. Lett.* **47**, 1400 (1981)